

ORIGINAL ARTICLE

Oncolytic measles viruses encoding interferon β and the thyroidal sodium iodide symporter gene for mesothelioma virotherapyH Li¹, K-W Peng¹, D Dingli^{1,2}, RA Kratzke³ and SJ Russell^{1,2}

¹Department of Molecular Medicine, Mayo Clinic, Rochester, MN, USA; ²Division of Hematology, Department of Surgery and Medicine, Mayo Clinic, Rochester, MN, USA and ³Departments of Surgery and Medicine, University of Minnesota Medical School, Minneapolis, MN, USA

Mesothelioma usually leads to death within 8–14 months of diagnosis. To increase the potency of oncolytic measles viruses (MVs) for mesothelioma therapy, we inserted the interferon β (IFN β) gene alone or with the human thyroidal sodium iodide symporter (NIS) gene into attenuated MV of the Edmonston lineage. The corresponding mouse IFN β (mIFN β) viruses, MV-mIFN β and MV-mIFN β -NIS, successfully propagated in human mesothelioma cells, leading to intercellular fusion and cell death. High levels of mIFN β were detected in the supernatants of the infected cells, and radioiodine uptake was substantial in the cells infected with MV-mIFN β -NIS. MV with mIFN β expression triggered CD68-positive immune cell infiltration 2–4 times higher than MV-GFP injected into the tumor site. The numbers of CD31-positive vascular endothelial cells within the tumor were decreased at day 7 after intratumoral injection of MV-mIFN β or MV-mIFN β -NIS, but not after MV-GFP and PBS administration. Immunohistochemical analysis showed that MV-mIFN β changed the microenvironment of the mesothelioma by increasing innate immune cell infiltration and inhibiting tumor angiogenesis. Oncolytic MVs coding for IFN β effectively retarded growth of human mesotheliomas and prolonged survival time in several mesothelioma tumor models. The results suggest that oncolytic MVs that code for IFN β and NIS will be potent and versatile agents for the treatment of human mesothelioma.

Cancer Gene Therapy (2010) 17, 550–558; doi:10.1038/cgt.2010.10; published online 9 April 2010

Keywords: mesothelioma; oncolytic measles virus; interferon; thyroidal sodium iodide symporter

Introduction

Malignant pleural mesothelioma occurs in the mesothelium, which normally reduces friction between the lung and chest wall during breathing.¹ Exposure to asbestos for as little as 1 or 2 months can disable normal pleural cells and result in mesothelioma years later.² The prognosis for malignant pleural mesothelioma is poor with currently available treatments—surgery, radiotherapy, and chemotherapy.^{3,4} The majority of patients die from the disease within 8–14 months after diagnosis.¹

Type I interferons (IFNs) have been shown to elicit an antitumor response through the immune system.^{5–7} IFNs have immunoregulatory effects on antibody production, natural killer and T-cell activation, macrophage function,^{8,9} and antiangiogenic properties.¹⁰ Several animal models have been used to test the antitumor efficacy of recombinant IFNs delivered by viral vectors.^{11–13} A phase I clinical trial was carried out to determine the safety and toxicities of intrapleural infusion of human IFN β

expressed by an adenoviral vector to treat malignant pleural mesothelioma.¹⁴ The adenoviral-IFN β vector was generally well tolerated and impressively antitumor immune responses were elicited in 7 of the 10 patients and included the detection of cytotoxic T cells.¹⁴

Attenuated measles virus (MV) of the Edmonston lineage has substantial antitumor activity through cell–cell fusion (syncytia formation) in multiple tumor cell types, but spares normal cells.¹⁵ The oncolytic specificity of MV of the Edmonston lineage results from its ability to discriminate the differential expression of CD46 in tumor cells and normal cells.^{16,17} The CD46 receptor is highly expressed in human mesothelioma cells, which makes mesothelioma a potentially attractive target for MV of the Edmonston lineage virotherapy.¹⁸ Recent advances in genetic engineering of MV allow insertion of therapeutic and diagnostic transgenes as well as complete retargeting of MV.¹⁹ These strategies have resulted in the generation of recombinant MVs, allowing noninvasive monitoring of viral replication and viral spread.^{20–22} In this study, novel oncolytic MVs coding for mouse IFN β (mIFN β) were constructed and rescued successfully. Our study objectives were to determine the efficacy of oncolytic MV therapy for the treatment of mesothelioma and to evaluate the influence of mIFN β on virotherapy.

Correspondence: Dr SJ Russell, Department of Molecular Medicine, Mayo Clinic, 200 First Street SW, Rochester, MN 55905, USA.

E-mail: sjr@mayo.edu

Received 4 September 2009; revised 2 November 2009; accepted 13 December 2009; published online 9 April 2010

Materials and methods

Cell lines and viruses

The engineered cell line 293-3-46 used for rescue was maintained in Dulbecco's modified Eagle medium supplemented with 10% fetal bovine serum (FBS) and Geneticin (1.2 mg ml^{-1}) (Invitrogen, Carlsbad, California).²³ Vero cells were maintained in Dulbecco's modified Eagle medium with 5% FBS. Mesothelioma cell lines H2596, H2373, and H513 were maintained in RPMI 1640 with 10% FBS. Mesothelioma cell lines REN, M30, and MSTO-211H were maintained in Dulbecco's modified Eagle medium with 10% FBS.

The mIFN β was amplified by polymerase chain reaction using the following primers: 5' ATCCCGAC GCGTACGCCACCATGAACAACAGGTGGATCCTC 3' (sense) and 5' ACGCGATCGCGAGACGTCAGTT CATCAGTTTTGGAAGTTTCTGG 3' (antisense). The MluI and AatII restriction sites used for cloning are underlined. The template plasmid for mIFN β polymerase chain reaction was kindly provided by Dr Glen N Barber from Department of Microbiology and Immunology and Sylvester Comprehensive Cancer Center, University of Miami School of Medicine. The plasmids containing MV backbone were routinely maintained in the laboratory. The purified polymerase chain reaction product was subcloned into plasmid p(+)MV-GFP after digestion with MluI and AatII (New England Biolabs, Ipswich, MA), replacing the GFP gene, to generate plasmid p(+)MV-mIFN β . The plasmid p(+)MV-mIFN β and p(+)MV-GFP-sodium iodide symporter (NIS) were cut by the restriction enzymes SacII and NotI. The religated plasmid pMV-mIFN β -NIS contained the mIFN β gene upstream of the nucleocapsid gene and the NIS gene downstream of the H protein gene. MVs were rescued as described earlier.²³ Cell-associated virus was released by freezing and thawing the cells twice in liquid nitrogen, and the cell lysates were cleared by centrifugation. For titration of virus stocks, serial logarithmic dilutions of the virus were used to infect Vero cells in 96-well plates, and the 50% tissue-culture infective dose (TCID₅₀ per ml) was determined 4 days later, as described earlier.¹⁹ One-step growth curves were determined by infecting Vero cells with MVs at a multiplicity of infection (MOI) of 3. Vero cells were seeded into six-well plates at a density of 1×10^5 cells per well and allowed to attach at 37 °C for 8 h. The medium was aspirated, and the cells were incubated with the recombinant viruses in 1 ml Opti-MEM (Invitrogen) for 2 h. After infection, the culture medium was changed to Dulbecco's modified Eagle medium with 5% FBS, and the cells were kept at 37 °C. At selected time points, supernatant and cells were collected and stored at -80 °C. The mIFN level in the supernatant was determined by ELISA kit from PBL Biomedical laboratories (Piscataway, New Jersey) according to the product manual.

In vitro ¹²⁵I uptake studies

Iodide uptake studies were performed as described earlier.²⁰ Briefly, cells (H513 or H2373; 1.5×10^5 cells

per well) were plated into 12-well plates. The next day, cells were incubated with MVs at an MOI of 0.1 or 1.0. After 2 h of incubation at 37 °C, cells were washed, and the medium was replaced with complete RPMI 1640 and incubated at 37 °C for 48 h before testing for ¹²⁵I uptake. All wells were incubated with an activity of 7×10^5 counts per minute ¹²⁵I. In controls, 100 mM KClO₄ was added to inhibit NIS-mediated iodide influx. Plates were incubated at 37 °C for 45 min and were lysed with 1 M NaOH, and the activity in the lysis buffer was determined using a γ counter. All data points were measured in triplicate and displayed as means.

In vivo studies

C.B-17-SCID or athymic nu/nu mice (Harlan Sprague Dawley, Indianapolis, Indiana) were used for animal studies. To establish peritoneal tumors, mice were injected intraperitoneally with 1×10^7 mesothelioma H2373 cells in 200 μ l PBS. For subcutaneous tumors, mice were implanted in the right flank with 1×10^7 mesothelioma H513 cells in 200 μ l PBS. Subcutaneous tumor growth was determined by caliper measurements in two dimensions, and the volume estimated using the formula: (shortest diameter)² \times (longest diameter) \times 0.52. When the tumors were palpable (that is reached a mean diameter 0.3–0.5 cm), the mice were injected intratumorally with MVs (2×10^6 TCID₅₀). Tumor imaging was performed serially at 3, 7, and 14 days post-virus treatment using a high-resolution micro-SPECT/CT system (X-SPECT; Gamma Medica-Ideas, Northridge, California). Before imaging, mice were injected with ¹²⁵I 100 μ Ci intraperitoneally and imaged 1 h later.^{21,24} Tumor responses were determined by serial measurements of tumor growth. Mice were killed if a tumor grew to >10% of the weight of a mouse, if a tumor ulcerated, or if a mouse was unable to eat or drink. All animal studies were approved by the Mayo Clinic Institutional Animal Care and Use Committee and performed according to Assessment and Accreditation of Laboratory Animal Care-approved guidelines.

Immunohistochemistry and quantitation

The nude mice bearing H513 tumors were killed on days 4 and 7 ($n = 3$ /group/time point) after virus administration. Tumors were harvested and snap frozen. Frozen 6- μ m sections (three sections for each tumor sample) were stained using primary antibody against CD68 diluted at 1:200 (ab53444; Abcam, Cambridge, Massachusetts) or primary antibody against CD31 diluted at 1:50 (550300; BD Biosciences Pharmingen, San Diego, California) (HRP-AEC Cell and Tissue Staining kits; R&D Systems, Minneapolis, Minnesota). Briefly, sections were fixed in cold acetone for 5 min, followed by pretreatment with 0.3% hydrogen peroxide for 20 min to inhibit endogenous peroxidase activity. Subsequently, sections were blocked with 2% horse serum for 30 min and incubated with the primary antibody for 1 h at room temperature. After rinsing with PBS, the sections were incubated for 30 min with a biotinylated second antibody, and color development was performed afterward according to the kit

manual. Staining intensity was converted into grayscale values using Image J software (National Institutes of Health, Bethesda, Maryland).²⁵ For the CD68-positive staining slides, the spots representing the CD68 cells were counted and calculated per 0.1 mm². For CD31-positive staining slides, the total area occupied by CD31-positive cells were estimated by setting a 'threshold' using Image J's thresholding tool. The percentage of CD31-positive area to the tumor covered area was calculated and subjected to statistical analysis.

Statistical analysis

The GraphPad Prism 4.0 program (GraphPad Software, San Diego, California) was used for data handling, analysis, and graphic representation. Survival curves were plotted according to the Kaplan–Meier method, and survival fraction across treatment groups was compared using log-rank test analyses.

Results

Generation and characterization of MV-mIFN β and MV-mIFN β -NIS

The cDNA encoding mIFN β was inserted as an additional transcriptional unit into a full-length infectious molecular clone of MV of the Edmonston lineage upstream of the nucleocapsid gene. The plasmids p(+)MV-mIFN β and p(+)MV-GFP-NIS were cut by the same restriction enzymes SacII and NotI. The religated plasmid p(+)MV-mIFN β -NIS contained the mIFN β gene upstream of the nucleocapsid gene and NIS gene downstream of the H protein gene (Figure 1a). The corresponding viruses (MV-mIFN β , MV-mIFN β -NIS) were rescued, using 293-3-46 cells as reported earlier.²³ Parallel one-step growth curves of rescued viruses were made to compare virus replication. Growth kinetics of the recombinant viruses was scarcely affected by the recombinant engineering (Figure 1b). High levels of mIFN β could be readily detected by quantitative enzyme-linked immunosorbent assay for IFN β in the culture supernatant (Figure 1c).

To check the infectivity of MVs on mesothelioma cells, several mesothelioma cell lines were seeded into 12-well plates and infected by MVs with one MOI. Pictures were taken 36 h after infection, and cell death was calculated after trypan blue staining at 24, 48, and 72 h post-infection. All the mesothelioma cell lines were susceptible to MV infection and formed syncytia. The H2596 and MSTO-211H cells were more sensitive to MV infection; cell viability decreased dramatically within 48 h. (Figure 1d).

MV-mIFN β and MV-mIFN β -NIS successfully propagated in human mesothelioma cells

To test the replication of oncolytic MVs in mesothelioma cells, M30 (Figures 2a and b) and H513 (Figures 2c and d) cells were infected with MVs with MOI of 1.0. Cell-associated progeny viruses were checked at different time points, and mIFN β levels in the supernatant were

measured (Figures 2b and d). The results showed all the MVs propagated in the mesothelioma cell lines. High levels of mIFN β were detected in the supernatant of mesothelioma cells after MV-mIFN β or MV-mIFN β -NIS infection. The results indicated that mIFN β expression did not affect the MVs' oncolytic ability to the mesothelioma *in vitro*.

To study whether the virally expressed NIS protein was functional in MV-mIFN β -NIS-infected cells, *in vitro* iodide uptake assays were performed, as described earlier.²⁰ Mesothelioma cell lines H513 and H2373 were infected with MV-mIFN β -NIS or MV-GFP-NIS. After incubation with ¹²⁵I, mesothelioma cells showed considerable iodide uptake, increasing with time because of virus replication and increasing NIS expression (Figures 3a and b). Iodide uptake was blocked by potassium perchlorate, a specific inhibitor of NIS. Cells infected with MV-mIFN β did not express NIS and did not concentrate radioiodine (Figures 3a and b). These uptake studies showed proof of virus-driven NIS protein expression and its proper targeting of the plasma membrane.

MV-mIFN β changed the mesothelioma tumor microenvironment

To determine the behavior of MV-mIFN β in the tumor environment, 1×10^7 H513 cells were injected subcutaneously into the flank of nude mice. When the tumors reached 5 mm in diameter, MVs were injected intratumorally. Tumor samples from different time points after viral injection were snap frozen and cut into 6- μ m sections. Anti-CD68 and anti-CD31 antibodies were used to detect the immune cell infiltration and vascular density changes after viral administration. Sections from different treatments were compared, and representative changes were recorded under $\times 200$ magnification (Figure 4a). The quantitative analyses were performed using ImageJ software with the same threshold.²⁵ At day 4, the numbers of CD68-positive cells were increased in the tumors with MVs administration. Over time, the CD68-positive cells increased more in the MV-mIFN β -treated samples than in the MV-GFP-treated tumors (Figure 4b). MV with mIFN β expression triggered CD68-positive immune cell infiltration at a frequency 2–4 times higher than that of the other MVs at day 7 after MV injection into the tumor site. Anti-CD31 antibody was used to stain vascular endothelial cells in the tumor site. The vascular densities in the MV-mIFN β -treated tumors were significantly different from the MV-GFP-treated ones at days 4 and 7 after the viral injections (Figure 4c). The results showed the obvious advantage of including IFN β in MV. The MV-mIFN β changed the mesothelioma tumor microenvironment by increased innate immune cell infiltration and inhibition of tumor angiogenesis.

In vivo ¹²⁵I update imaging of MV-mIFN β -NIS

The NIS gene has been used to monitor viral replication *in vivo* in different tumor models.^{20–22,24} To determine whether mIFN β affects NIS expression *in vivo*, H513 mesotheliomas were established subcutaneously in female

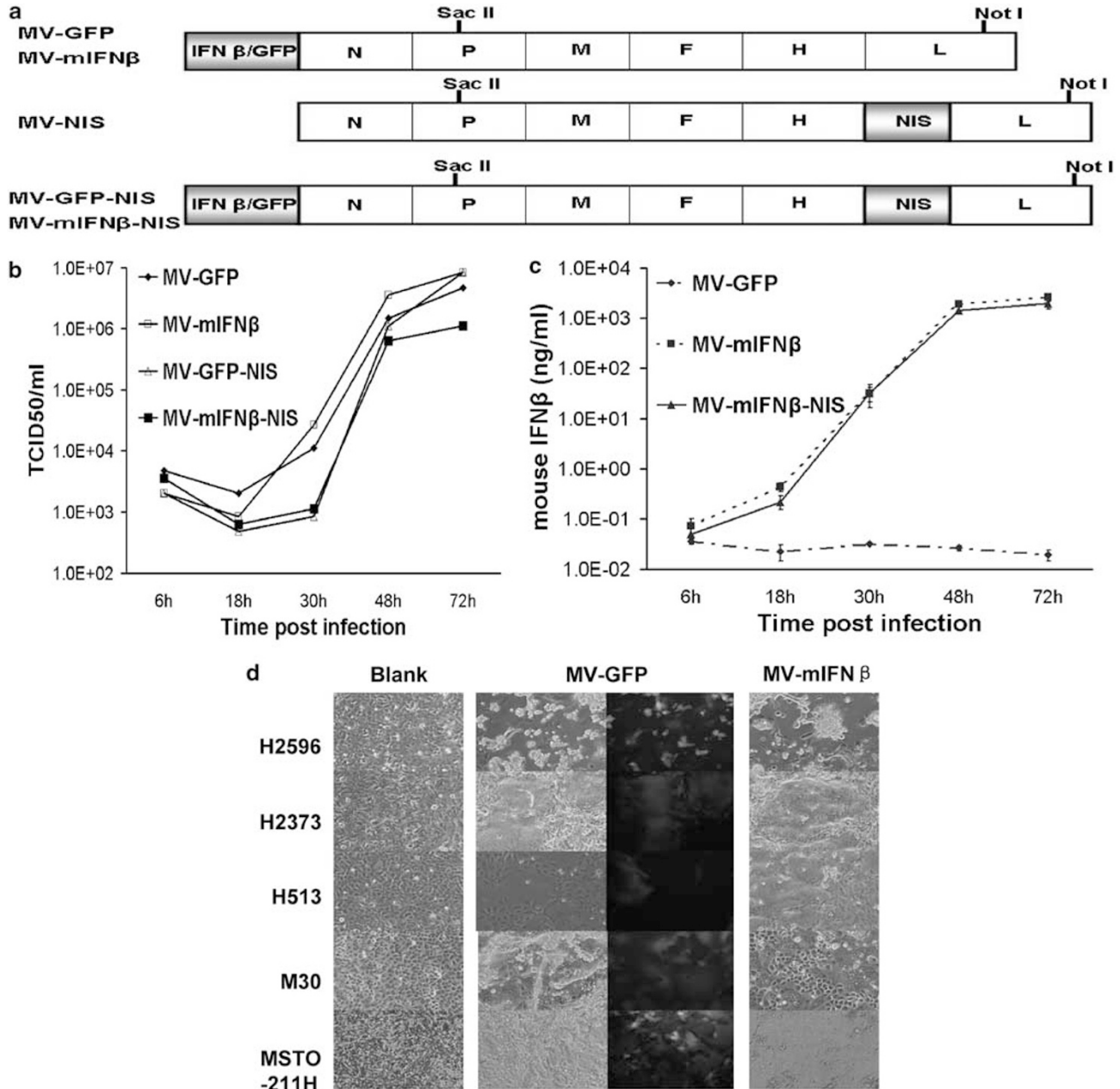


Figure 1 Characterization of MVs *in vitro*. Schematic construction of MV-mIFNβ and MV-mIFNβ-NIS is shown in (a). mIFNβ gene was cloned to take place of the GFP gene in MV genome. p(+)MV-mIFN and p(+)MV-NIS were cut by the same pair of restriction enzymes and religated to contain both the mIFN and NIS gene in the MV genome (a). One-step viral growth curves for MV-GFP, MV-mIFNβ, MV-GFP-NIS, and MV-mIFNβ-NIS in Vero cells (b). Supernatants from the culture were collected to measure mIFNβ secretion (c). Human mesothelioma cells were infected by MVs. Human mesothelioma cells H2596, H2373, H513, M30, and MSTO-211H were infected with MV-GFP or MV-mIFNβ at MOI of 1.0. Pictures were taken 36 h later (d).

C.B-17-SCID mice. When the tumors reached a mean diameter of 0.5 cm, the mice were injected intratumorally with MVs (2×10^6 TCID50). After 3 days, the mice were injected with ^{125}I (100 μCi) and underwent CT/SPECT imaging 1 h later. The imaging procedure was repeated on days 7 and 14 after virus administration. Viral gene expression and viral replication are tightly coupled. All images were acquired 1 h after injection of the same dose of ^{125}I (100 μCi) and adjusted for the same image

intensity. Thus, serial iodide uptake by the tumors should reflect increasing NIS expression and, therefore, serve as a surrogate for MV replication. As expected, there was no γ photon signal from the mesothelioma xenografts in mice injected with MV-GFP or MV-mIFNβ because no iodide uptake occurred (Figure 5). MV-GFP-NIS- or MV-mIFNβ-NIS-treated tumors concentrated radioiodine and MV gene expression were readily visualized by imaging at day 7 (Figure 5). This imaging study showed

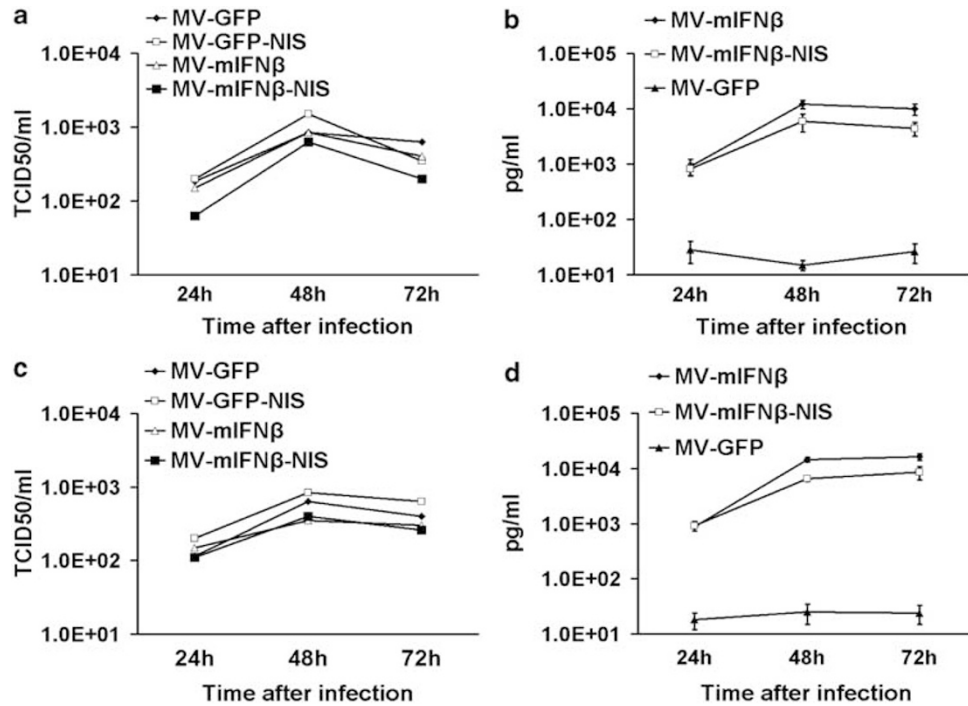


Figure 2 Virus progeny and mIFN β secretion by human mesothelioma cells after infection with MVs. M30 mesothelioma cells were infected by MVs at MOI of 1.0. After 24, 48, or 72 h of incubation, cells were harvested for virus titration (a), and supernatant was collected to measure the mIFN β secretion (b). The same experiments were performed to the human mesothelioma cells H513 for viral progeny (c) and mIFN β (d).

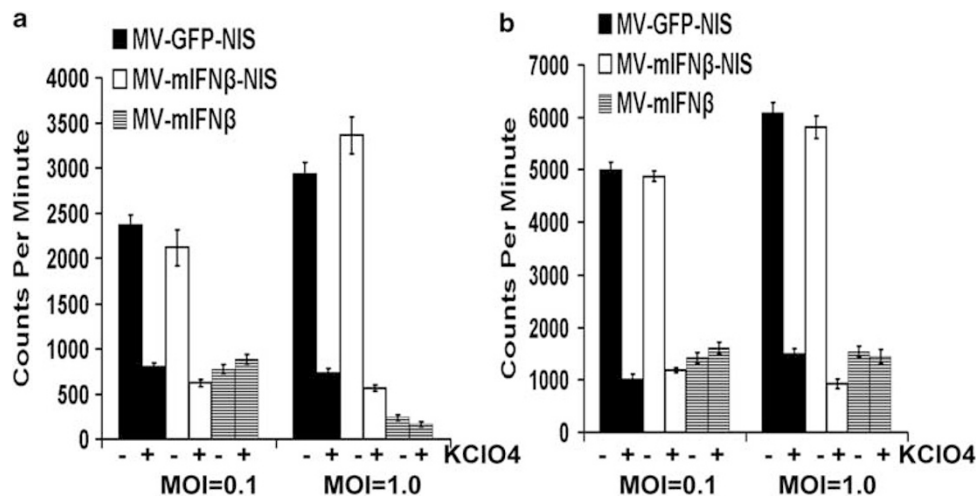


Figure 3 ¹²⁵I uptake by human mesothelioma cells after infection with MVs. Mesothelioma cells were incubated with MVs at MOI of 1.0 or 0.1 for 48 h. Uptake of ¹²⁵I was assayed in mesothelioma H513 (a) and H2373 (b). Iodide uptake is blocked by perchlorate, a specific inhibitor of NIS. Without NIS, cells infected with MV-mIFN β do not concentrate iodide.

that the human thyroidal NIS could facilitate noninvasive *in vivo* monitoring of MV-mIFN β -NIS propagation by radioiodine imaging.

mIFN β increased the potency of MVs in vivo for killing xenografted mesotheliomas

The antitumor activity of MV has been demonstrated against a variety of tumor xenografts in mice.¹⁵ However,

MVs have not yet been used to treat mesotheliomas *in vivo*. To test the efficacy of MVs, 1×10^7 mesothelioma H513 cells were injected into the flanks of nude mice. Two weeks later, when the tumors had grown to a diameter of 5 mm, MV or PBS was injected intratumorally, and tumor growth was monitored twice a week. The survival curve was plotted at the end of the experiments. In control mice, rapid tumor growth was observed, whereas tumor growth

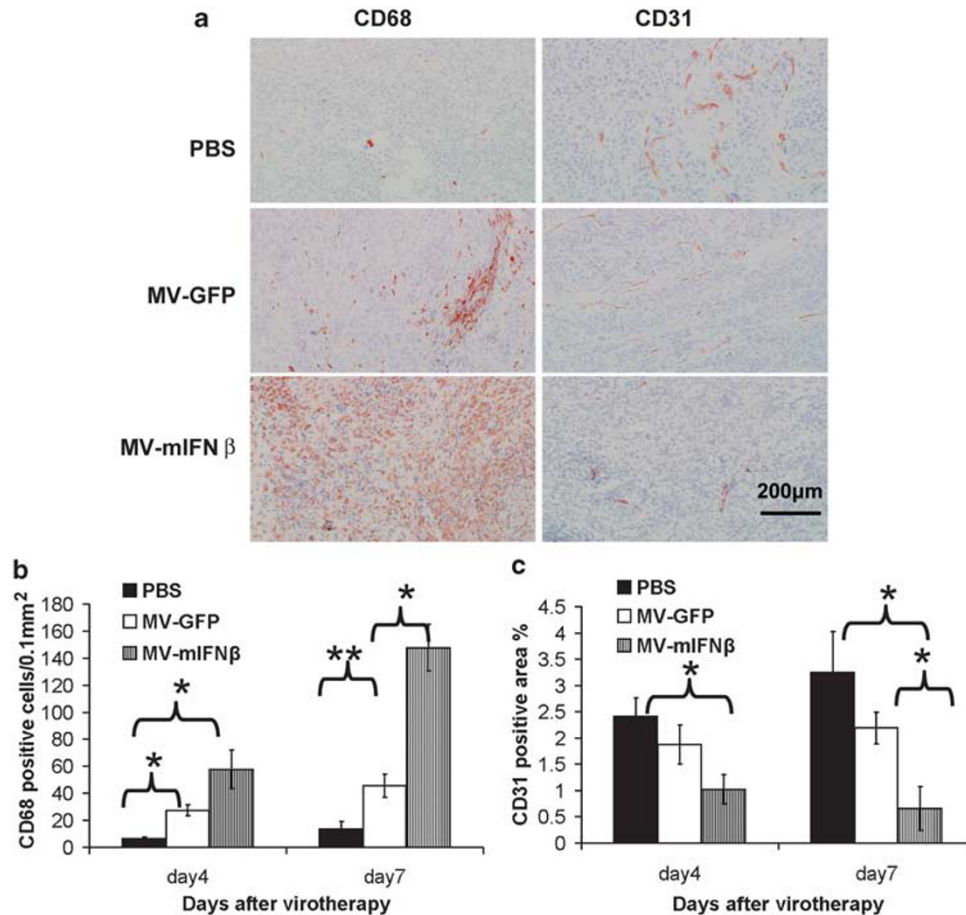


Figure 4 Administration of MV-mIFN β increased infiltration of CD68-positive immune cells and inhibition of tumor angiogenesis. mIFN β induced robust CD68-positive cell infiltration and decreased microvessel density (as indicated by CD31 staining) in the tumor. Mesothelioma H513-bearing nude mice were given PBS, MV-GFP, or MV-mIFN β intratumorally; (a) 4 or 7 days later, tumor sections were stained for CD68+ and CD31+ cells. Original magnification, $\times 200$. Quantitative analysis was carried out to compare CD68+ infiltration into 0.1 mm² area (b), and the CD31 coverage rate was calculated (c) as described in Material and methods. * $P < 0.05$; ** $P < 0.01$. Scale bar denotes 200 μm (a, right corner).

was arrested in mice treated with MVs. Both MV-GFP and MV-GFP-NIS had the similar antitumor efficacy against H513 and controlled tumor growth (Figure 6a). The median survival of control animals receiving PBS was 20 days after tumor engraftment, whereas the median survival was 45 days for mice receiving MV-GFP or MV-GFP-NIS ($P < 0.001$) and 65 days for those receiving MV-mIFN β or 60 days for those receiving MV-mIFN β -NIS ($P < .001$) (Figure 6b). Thus, MV-mIFN β and MV-mIFN β -NIS significantly reduced tumor burden and lengthened survival time.

The mesothelioma cell line H513 was established the same way in SCID mice. About 2 weeks later, when the tumor reached a diameter of 5 mm, the same treatments were applied to the mice. The tumor growth curve showed that administration of MV-mIFN β delayed tumor growth more than MV-GFP. The survival curve revealed the increased potency of MV-mIFN β to treat the mesothelioma (Figure 6c). To mimic orthotropic mesothelioma in human beings, 1×10^7 H2373 cells were injected into peritoneum of nude mice. Four weeks later, MVs (2×10^6

TCID₅₀) were injected into the peritoneum. The morbidity and mortality were monitored and survival curves were plotted. As shown in Figure 6d, MV-mIFN β administration resulted in long-term protection of mice from the mesothelioma (Figure 6d).

The *in vivo* study results suggested that the oncolytic MVs will be potent and versatile agents for the treatment of human mesothelioma and the inclusion of IFN β may increase the efficiency.

Discussion

Several oncolytic viruses have been used experimentally to treat tumors, such as adenovirus, vesicular stomatitis virus, herpes simplex virus, Newcastle disease virus, and vaccinia viruses as well as MV.^{26–28} MV is representative of a new generation of safe and effective oncolytic viruses.¹⁵ Spontaneous tumor regression has occurred during natural measles infection.²⁹ The MVs can be

engineered to enhance their tumor specificity, increase their antitumor potency, and facilitate noninvasive *in vivo* monitoring of their spread.¹⁵ Live attenuated MVs have been used to treat several human tumors such as multiple myeloma,¹⁷ glioma,³⁰ ovarian carcinoma,³¹ pancreatic

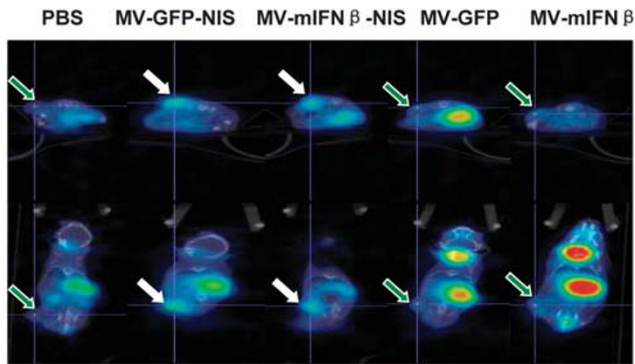


Figure 5 ¹²⁵I uptake images of mesothelioma-bearing mice treated with MVs intratumorally. Mesothelioma H513-bearing SCID mice were treated with MVs intratumorally. On day 7, ¹²⁵I was used to check iodine uptake. Mice were imaged with CT/SPECT 1 h after ¹²⁵I intraperitoneal injection. There was significant uptake of ¹²⁵I in MV-GFP-NIS or MV-mIFN β -NIS-treated mesothelioma xenografts (white arrow). The pictures were taken at the section with the peak ¹²⁵I uptake in the tumor. In contrast, MV-GFP, MV-mIFN β , and PBS-treated tumors had much less signals (green arrow). The different physiologic uptake in thyroid gland and stomach and excretion into bladder were observed.

cancer,²¹ and prostate cancer.³² Recently, a live attenuated MV was evaluated to kill mesothelioma cells *in vitro*.¹⁸ Together with our results, it is evident that MV could kill malignant pleural mesothelioma cells and spare nontransformed mesothelial cells by causing syncytia in tumor cells. The *in vivo* data from this study showed further efficacy of oncolytic MVs for the xenografted mesothelioma in mice. In addition to the 50-year record of safe MV use as a vaccine, MVs have the potential to be applied to mesothelioma therapy in clinic safely and effectively.

Type I IFNs delivered in the form of proteins have been explored in cancers.³³ The limited efficacy is due to the short half-life of the protein (<60 min) and nonspecific binding to tissues other than the tumor. To improve type I IFN therapy, gene transfer methods such as plasmids or various viral vectors (for example adenovirus) have been tried in tumor models such as lung cancer, prostate cancer, and glioma.^{11,34–36} Adenoviral vector expressing IFN β has been used extensively to treat mesothelioma in a mouse model, and a clinical phase 1 trial has proved its safety and responsiveness in mesothelioma patients.¹⁴ Vesicular stomatitis virus was engineered to express IFN β , which was significantly attenuated compared with wild-type vesicular stomatitis virus and retained oncolytic activity against metastatic lung disease in immunocompetent animals.³⁷ To exploit defects in mechanisms of cancer host defense, the IFN gene was cloned into vaccinia virus and selective tumor killing was achieved after systemic delivery.³⁸ This study provides another vector platform

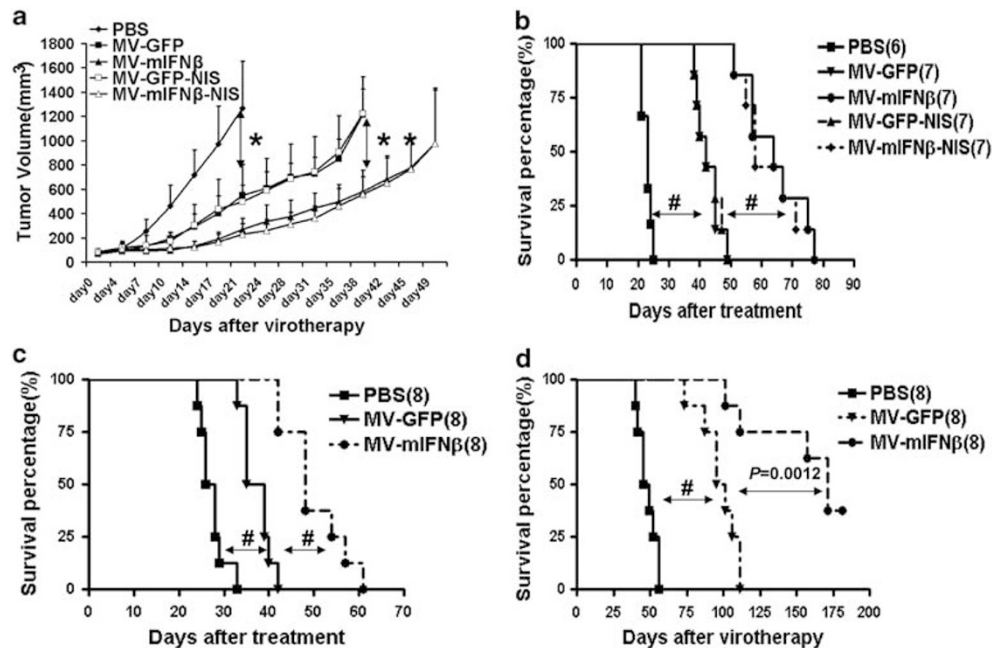


Figure 6 Therapeutic effects of oncolytic MVs for mesothelioma xenografts. Mesothelioma H513 cells were inoculated into the flanks of nude mice. The efficacy of MVs was compared by tumor growth (a) and survival (b). MV with mIFN β expression arrested tumor growth. The experiment was repeated in SCID mice bearing mesothelioma H513 cells. Both tumor growth (data not shown) and survival (c) showed the superiority of MV-mIFN β . Mesothelioma H2373 cells were established in the peritoneum of nude mice to mimic the human conditions. MV-mIFN β significantly extended the survival of mice (d). * $P < 0.05$; ** $P < 0.01$; # $P < 0.001$.

for type I IFN to treat mesotheliomas. Although type I IFN has been shown to have great antitumor effect, when delivered by viral vectors, IFN may also induce a strong immune response against the vector itself. In this study, by inclusion of mIFN β , MV-mIFN β showed the increased potency of MVs *in vivo*. Compared with MV-GFP-treated tumor samples, MV-mIFN β -treated tumor sections showed accumulated immune cell infiltration and decreased vascular density. Imaging studies showed that NIS expression was not markedly affected by inclusion of mIFN β in the MV vector in the SCID mice model 7 days after the viral treatment. Presumably, IFN β will interfere with MV replication more severely in immune competent mice. However, the overall outcome in this study is that MV-mIFN β slows tumor growth and lengthens survival.

The imaging platform using the NIS gene offers a convenient approach to monitor oncolytic MV replication noninvasively *in vivo*. NIS expression within a tumor could be affected by several factors such as tumor size, the rate of viral propagation, and the rate of viral clearance in the host. Serial imaging was performed in SCID mice bearing subcutaneous mesotheliomas on days 3, 7, and 14 after MV administration. A specific signal was detected in the mesotheliomas after injection of MV-GFP-NIS or MV-mIFN β -NIS, but not in the control groups, allowing us to attribute the tumor-specific signal to virus-driven expression of the NIS gene. The iodine uptake in the tumors could be picked up at days 3 and 7 after MV-GFP-NIS or MV-mIFN β -NIS administration. However, at day 14, it is weaker in the MV-mIFN β -NIS-treated tumors than in the MV-GFP-NIS-treated ones. We speculated that the MV-mIFN β -NIS replicated at the similar rate as the MV-GFP-NIS within tumor for at least 7 days after viral injection, allowing the MV-mIFN β enough time to destroy the tumor more effectively than the MV-GFP. The data also suggest that immune responses induced by mIFN β not only lead to antitumor effects, but also cause faster viral clearance. Several preclinical studies have shown the ablative effects of ^{131}I in tumor xenografts,^{20,32,39,40} which suggests that NIS may be a potent tool to combine with radiotherapy for treatment of mesothelioma.

Conclusion

In rodent mesothelioma models, we determined that MVs expressing mIFN β could increase innate immune cell infiltration and inhibit tumor angiogenesis more efficiently than the parental virus. Therapeutic activity was enhanced by the IFN transgene, whereas the NIS transgene permitted noninvasive monitoring of intratumoral virus spread by radioiodine imaging.

Conflict of interest

Stephen J Russell is a named inventor on patents pertaining the use of Measles Virus as an anticancer drug therapy. These patents are owned by Mayo Clinic.

Acknowledgements

The project was funded by Schulze Family Foundation, Minnesota Partnership for Biotechnology and Medical Genomics and the National Institutes of Health (CA100634). We thank Dr Steven M Albelda (University of Pennsylvania) for kindly providing the REN, M30, and MSTO-211H cells.

References

- 1 Robinson BW, Musk AW, Lake RA. Malignant mesothelioma. *Lancet* 2005; **366**: 397–408.
- 2 Neri M, Ugolini D, Dianzani I, Gemignani F, Landi S, Cesario A *et al*. Genetic susceptibility to malignant pleural mesothelioma and other asbestos-associated diseases. *Mutat Res* 2008; **659**: 126–136.
- 3 Vogelzang NJ. Chemotherapy for malignant pleural mesothelioma. *Lancet* 2008; **371**: 1640–1642.
- 4 Muers MF, Stephens RJ, Fisher P, Darlison L, Higgs CM, Lowry E *et al*. Active symptom control with or without chemotherapy in the treatment of patients with malignant pleural mesothelioma (MS01): a multicentre randomised trial. *Lancet* 2008; **371**: 1685–1694.
- 5 Kantarjian HM, Talpaz M, O'Brien S, Jones D, Giles F, Garcia-Manero G *et al*. Survival benefit with imatinib mesylate versus interferon-alpha-based regimens in newly diagnosed chronic-phase chronic myelogenous leukemia. *Blood* 2006; **108**: 1835–1840.
- 6 Ravandi F, Estrov Z, Kurzrock R, Breitmeyer JB, Maschek BJ, Talpaz M. A phase I study of recombinant interferon-beta in patients with advanced malignant disease. *Clin Cancer Res* 1999; **5**: 3990–3998.
- 7 Ravandi F, Rytting ME, Osmon C, Braud EL, Roach RW, Edwards K *et al*. Phase II trial of 5-fluorouracil, folinic acid and recombinant alpha-2a-interferon in patients with advanced colorectal cancer. *Anticancer Drugs* 1999; **10**: 519–524.
- 8 Chan CW, Crafton E, Fan HN, Flook J, Yoshimura K, Skarica M *et al*. Interferon-producing killer dendritic cells provide a link between innate and adaptive immunity. *Nat Med* 2006; **12**: 207–213.
- 9 Le Bon A, Tough DF. Links between innate and adaptive immunity via type I interferon. *Curr Opin Immunol* 2002; **14**: 432–436.
- 10 Brem H, Gresser I, Grosfeld J, Folkman J. The combination of antiangiogenic agents to inhibit primary tumor growth and metastasis. *J Pediatr Surg* 1993; **28**: 1253–1257.
- 11 Natsume A, Tsujimura K, Mizuno M, Takahashi T, Yoshida J. IFN-beta gene therapy induces systemic antitumor immunity against malignant glioma. *J Neurooncol* 2000; **47**: 117–124.
- 12 Qin XQ, Tao N, Dergay A, Moy P, Fawell S, Davis A *et al*. Interferon-beta gene therapy inhibits tumor formation and causes regression of established tumors in immune-deficient mice. *Proc Natl Acad Sci USA* 1998; **95**: 14411–14416.
- 13 Wilderman MJ, Sun J, Jassar AS, Kapoor V, Khan M, Vachani A *et al*. Intrapulmonary IFN-beta gene therapy using an adenoviral vector is highly effective in a murine orthotopic model of bronchogenic adenocarcinoma of the lung. *Cancer Res* 2005; **65**: 8379–8387.
- 14 Serman DH, Recio A, Carroll RG, Gillespie CT, Haas A, Vachani A *et al*. A phase I clinical trial of single-dose

- intrapleural IFN-beta gene transfer for malignant pleural mesothelioma and metastatic pleural effusions: high rate of antitumor immune responses. *Clin Cancer Res* 2007; **13**: 4456–4466.
- 15 Blehacz B, Russell SJ. Measles virus as an oncolytic vector platform. *Curr Gene Ther* 2008; **8**: 162–175.
 - 16 Anderson BD, Nakamura T, Russell SJ, Peng KW. High CD46 receptor density determines preferential killing of tumor cells by oncolytic measles virus. *Cancer Res* 2004; **64**: 4919–4926.
 - 17 Ong HT, Timm MM, Greipp PR, Witzig TE, Dispenzieri A, Russell SJ *et al*. Oncolytic measles virus targets high CD46 expression on multiple myeloma cells. *Exp Hematol* 2006; **34**: 713–720.
 - 18 Gauvrit A, Brandler S, Sapede-Peroz C, Boisgerault N, Tangy F, Gregoire M. Measles virus induces oncolysis of mesothelioma cells and allows dendritic cells to cross-prime tumor-specific CD8 response. *Cancer Res* 2008; **68**: 4882–4892.
 - 19 Nakamura T, Peng KW, Harvey M, Greiner S, Lorimer IA, James CD *et al*. Rescue and propagation of fully retargeted oncolytic measles viruses. *Nat Biotechnol* 2005; **23**: 209–214.
 - 20 Dingli D, Peng KW, Harvey ME, Greipp PR, O'Connor MK, Cattaneo R *et al*. Image-guided radiotherapy for multiple myeloma using a recombinant measles virus expressing the thyroidal sodium iodide symporter. *Blood* 2004; **103**: 1641–1646.
 - 21 Carlson SK, Classic KL, Hadac EM, Dingli D, Bender CE, Kemp BJ *et al*. Quantitative molecular imaging of viral therapy for pancreatic cancer using an engineered measles virus expressing the sodium-iodide symporter reporter gene. *AJR Am J Roentgenol* 2009; **192**: 279–287.
 - 22 Myers RM, Greiner SM, Harvey ME, Griesmann G, Kuffel MJ, Buhrow SA *et al*. Preclinical pharmacology and toxicology of intravenous MV-NIS, an oncolytic measles virus administered with or without cyclophosphamide. *Clin Pharmacol Ther* 2007; **82**: 700–710.
 - 23 Radecke F, Spielhofer P, Schneider H, Kaelin K, Huber M, Dotsch C *et al*. Rescue of measles viruses from cloned DNA. *EMBO J* 1995; **14**: 5773–5784.
 - 24 Carlson SK, Classic KL, Hadac EM, Bender CE, Kemp BJ, Lowe VJ *et al*. *In vivo* quantitation of intratumoral radioisotope uptake using micro-single photon emission computed tomography/computed tomography. *Mol Imaging Biol* 2006; **8**: 324–332.
 - 25 Rasband WS. ImageJ. <http://rsb.info.nih.gov/ij/>, U.S. National Institutes of Health: Bethesda, Maryland, USA, 1997–2008.
 - 26 Parato KA, Senger D, Forsyth PA, Bell JC. Recent progress in the battle between oncolytic viruses and tumours. *Nat Rev Cancer* 2005; **5**: 965–976.
 - 27 Russell SJ, Peng KW. Viruses as anticancer drugs. *Trends Pharmacol Sci* 2007; **28**: 326–333.
 - 28 Kelly E, Russell SJ. History of oncolytic viruses: genesis to genetic engineering. *Mol Ther* 2007; **15**: 651–659.
 - 29 Bluming AZ, Ziegler JL. Regression of Burkitt's lymphoma in association with measles infection. *Lancet* 1971; **2**: 105–106.
 - 30 Allen C, Paraskevaku G, Liu C, Iankov ID, Msaouel P, Zollman P *et al*. Oncolytic measles virus strains in the treatment of gliomas. *Expert Opin Biol Ther* 2008; **8**: 213–220.
 - 31 Hasegawa K, Pham L, O'Connor MK, Federspiel MJ, Russell SJ, Peng KW. Dual therapy of ovarian cancer using measles viruses expressing carcinoembryonic antigen and sodium iodide symporter. *Clin Cancer Res* 2006; **12**: 1868–1875.
 - 32 Msaouel P, Iankov ID, Allen C, Morris JC, von Messling V, Cattaneo R *et al*. Engineered measles virus as a novel oncolytic therapy against prostate cancer. *Prostate* 2009; **69**: 82–91.
 - 33 Christmas TI, Manning LS, Garlepp MJ, Musk AW, Robinson BW. Effect of interferon-alpha 2a on malignant mesothelioma. *J Interferon Res* 1993; **13**: 9–12.
 - 34 Sakurai F, Terada T, Maruyama M, Watanabe Y, Yamashita F, Takakura Y *et al*. Therapeutic effect of intravenous delivery of lipoplexes containing the interferon-beta gene and poly I: poly C in a murine lung metastasis model. *Cancer Gene Ther* 2003; **10**: 661–668.
 - 35 Cao G, Su J, Lu W, Zhang F, Zhao G, Marteralli D *et al*. Adenovirus-mediated interferon-beta gene therapy suppresses growth and metastasis of human prostate cancer in nude mice. *Cancer Gene Ther* 2001; **8**: 497–505.
 - 36 Natsume A, Mizuno M, Ryuke Y, Yoshida J. Antitumor effect and cellular immunity activation by murine interferon-beta gene transfer against intracerebral glioma in mouse. *Gene Ther* 1999; **6**: 1626–1633.
 - 37 Obuchi M, Fernandez M, Barber GN. Development of recombinant vesicular stomatitis viruses that exploit defects in host defense to augment specific oncolytic activity. *J Virol* 2003; **77**: 8843–8856.
 - 38 Kirn DH, Wang Y, Le Boeuf F, Bell J, Thorne SH. Targeting of interferon-beta to produce a specific, multi-mechanistic oncolytic vaccinia virus. *PLoS Med* 2007; **4**: e353.
 - 39 Boland A, Ricard M, Opolon P, Bidart JM, Yeh P, Filetti S *et al*. Adenovirus-mediated transfer of the thyroid sodium/iodide symporter gene into tumors for a targeted radiotherapy. *Cancer Res* 2000; **60**: 3484–3492.
 - 40 Cho JY, Shen DH, Yang W, Williams B, Buckwalter TL, La Perle KM *et al*. *In vivo* imaging and radioiodine therapy following sodium iodide symporter gene transfer in animal model of intracerebral gliomas. *Gene Ther* 2002; **9**: 1139–1145.



This work is licensed under the Creative Commons Attribution-NonCommercial-No Derivative Works 3.0 License. To view a copy of this license, visit <http://creativecommons.org/licenses/by-nc-nd/3.0/>